International Journal of Applied Science and Engineering

Vibration analysis of nano-composite plate based on HSPT and numerical analysis

Rasha Mohammed Hussein*

Mechanical Engineering Department, University of Technology, Iraq

ABSTRACT

The most interested point is to find the natural frequency of a nano-composites plate and its study analytically and numerically by ANSYS software. Very good mechanical properties of carbon nanotubes give them importance for reinforcing the composite plate to get acceptable property for a new material. The Polyprime EP epoxy as a matrix, which is strengthened via Multi-Walled Carbon Nanotubes (MWCNTs), has been analyzed. Three loading ratios (0.1, 0.5 and 1 wt.%) of MWCNTs have been added to epoxy using a magnetic stirrer, and then hardener was added and blended with them. Tensile tests were conducted upon unfilled, MWCNT-filled epoxy to find the materials' mechanical properties. A CNC machine was used to cut all samples. Scanning Electron Microscopy (SEM) was utilized to obtain the nanotubes' dispersal status into the base matrix. Higher Order Shear Deformation Plate Theory (HSDT) and ANSYS software were employed for finding the natural frequency for the three loading ratios. The results of tensile tests manifested an enhancement in the Young's modulus for higher supplement percentages of MWCNT. And, the maximum tensile strength was obtained at 0.5 wt.% of MWCNT with the ratio 66.7%. The SEM images explicated that the sample of 0.1 wt.% MWCNT possesses less voids in comparison with the other samples. The effect of increasing loading ratio from 0.1 wt.% to 0.5 wt.% increased the frequency by 5.9%.

Keywords: Multi-walled carbon nanotubes (MWCNT), Epoxy composites, Vibration, Higher order shear deformation plate theory (HSPT).

OPEN ACCESS

Received: January 6, 2023
Revised: March 3, 2023
Accepted: March 13, 2023

Corresponding Author:
Rasha Mohammed Hussein
Rasha.M.Hussein@uotechnology.edu.iq

Copyright: The Author(s). This is an open access article distributed under the terms of the Creative Commons Attribution License (CC BY 4.0), which permits unrestricted distribution provided the original author and source are cited.

Publisher:
Chaoyang University of Technology
ISSN: 1727-2394 (Print)
ISSN: 1727-7841 (Online)

1. INTRODUCTION

Performance of the polymer materials can be considerably improved by adding small amount of inorganic substances, like carbon nanotubes (CNTs) to the polymer matrix, and then the final material is called nanocomposites material (Ebrahimi, 2012; Parameswaranpillai et al., 2016). Plates are broadly utilized in the engineering structures, like the wings of aircraft and the structure of vehicles. Many studies have been investigated upon the mechanical conducts and plates' free vibration owing to their high the structural safety (Chakravety, 2008). Bending, buckling, forced and free vibration characteristics of a nonlocal nano-composite plate utilized the Third-order Shear Deformation Theory (TSDT) were studied by Mohammadimehr and Rostami (2017) by driving the governing differential equations employing the principle Hamilton and the equations of Maxwell. The fundamental frequency and crucial buckling load increased with the rising of the $CoFe_2O_4$-$BaTiO_3$ fraction and decreasing the amplitude vibration. Classic theory of plate was used, for investigating the buckling as well as the free vibration of isotropic nano plate by employing both Pasternak-type and Winkler-type foundation models to find the elastic matrix, by Bastami and Behjat (2017). Single-Walled Carbon Nanotubes (SWCNTs) in amorphous polyethylene were analyzed with the First-order Shear Deformation Theory (FSDT), CLPT, and HSPT to calculate the fundamental frequencies. The properties of the composite were calculated using the Multiscale Finite Element Method (FEM). The increasing of CNTs volume

fractions led to increase the stiffness of the plate (Safaei et al., 2019).

The FEM was conducted to find the vibrational features of polymer matrix composite plates that are strengthened by both CNTs and carbon fibers (CFs). The vibrational behavior of composite rectangular plates was investigated with clamped and simply supported conditions. It was shown that the amplitude decreased when both CNTs and CFs were infused into the polymer (Ahmadi et al., 2019). Ebrahimi and Dabbagh (2019) studied the natural vibration of multi-scale hybrid nano-composites. The structure is made of macro- and nano- reinforcement's CNTs and carbon fiber (CF) and that are infused into an epoxy matrix. The classical theory of plates was derived using Hamiltonian approach and then solving the problem by Galerkin's method. The fundamental frequency of hybrid plates can be duplicated via either infusing the volume fraction of CFs or using higher weight fractions of CNT. Damping ratios and natural frequencies of nano-composite beams with different CNT weight ratios and glass fibres were examined by Hocaoğlu and Karagülle (2020), the samples which were cut in parallel and perpendicular directions showed an increasing in the natural frequency, and the damping ratio of the parallel sample increased. Bouazza and Zenkour (2020) presented analytically the free vibration of nanocomposite plates reinforced by SWCNTs utilizing the simplified two-variable nth-higher-order theory solved by Navier solution. The forced vibration of a simply supported nanocomposite beam subjected to a harmonic point load at the center of beam analyzed by the first-order shear deformation beam theory and solved with Ritz method was studied. The results found that the increasing in the volume fractions of CNTs gave a rise in the amplitudes of vibration (Civalek et al., 2021). A novel method of superposition has been developed for plate for the free vibration with mixed boundary conditions. The analytic solution was based on Hamiltonian system governing equation, and the fundamental frequency results were obtained using non-Lévy-type plates for clamped and simply support edge (Xu et al., 2021). Nanoplates and nanoshells were vibrational analyzed to find the natural frequency including length scale effects employing the Hamilton's variation principle. The theory of higher-order nonlocal strain gradient was derived, and the proportional relations were found among volume fraction, size-length, and microstructure scales with the frequencies (Melaibari et al., 2022). Also, the FEM for temperature effect on the natural frequency of stiffened nanocomposite plate for different boundary conditions was examined by Maji et al. (2022) and showed a decreasing in natural frequencies due to the temperature increasing.

The modal analysis of functionally graded graphene platelets strengthened composite beams partially fluid contact was presented with the theory of first-order shear deformation for different dimensions, weight fractions, fluids (density and depth) and beam geometries Wu et al. (2022). And, the applications in damping of nano-composite beams that are made from epoxy resin reinforced with CNTs and GNPs was studied, and the finding was the peak value of the beams loss factor with a GNP reinforcement of 62.2% higher than the beam with the CNTs (Pan et al., 2022).

The aim of the current research is to study the influence of supplementing MWCNTs for three weight ratios on the mechanical and free vibration characteristics of epoxy/MWCNTs plates, where this point was not studied in the above literature. The MWCNTs's weight ratios (0.05, 0.1 and 0.5 wt.%) were manufactured by a magnetic stirrer. Tensile tests and SEM were performed. HSPT and ANSYS software were used to find the effect of the three loading ratios on the natural frequency for different loading ratios, aspect ratios, and thickness ratios.

2. EXPERIMENTAL WORK

2.1 Materials Preparations

Polyprime (EP) produced via Henkel Polybit Industries Ltd. with a hardener is employed as a matrix. MWCNTs utilized here with purity more than 90%, and the range of tube diameter and tube length are from 10 to 30 nm and from 10 to 30 μm, respectively.

Three samples of nano-composites were prepared with various weight contents of MWCNTs as 0.1, 0.5 and 1 wt.% via a magnetic stirrer depicted in Fig. 1. The resin was preheated to 59°C in the magnetic stirrer to decrease its viscosity that led to reduce the chance of voids initiated during mixing the epoxy and hardener and to provide a virtuous blending with nano carbon. After that, the MWCNTs were induced and blended for about 15 min to obtain homogeneity and then for 5 min approximately for mixing after the hardener additions. The resulted mix was poured into glass molds covered by overhead paper for preventing the adhesion for 24 h at the room temperature.

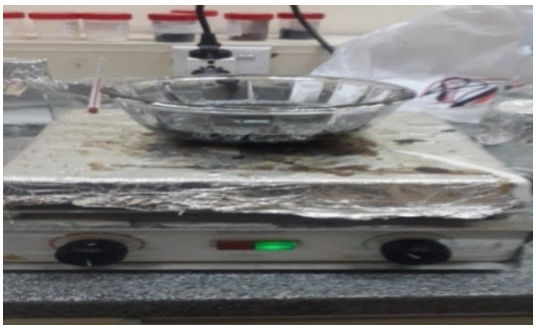

Fig. 1. Magnetic stirrer

2.2 Scanning Electron Microscope (SEM)

SEM (Inspect S50) is used to manifest the distribution of nano carbon tube in the epoxy. The SEM images of the epoxy/MWCNTs composites at various magnifications were scanned as in Fig. 2 for three weight ratios. From this figure, it can be seen that the plate with 0.1 wt.% CNTs

possesses fewer voids. The micro agglomeration particles appeared as black regions, where the pores with dark region are located at the junctions of agglomerates. The lighter regions are for epoxy matrix. Furthermore, the porosity is decreased by increasing the nano carbon because of the raising of agglomeration. It is clear that the crack propagation occurred near the voids in the microstructure.

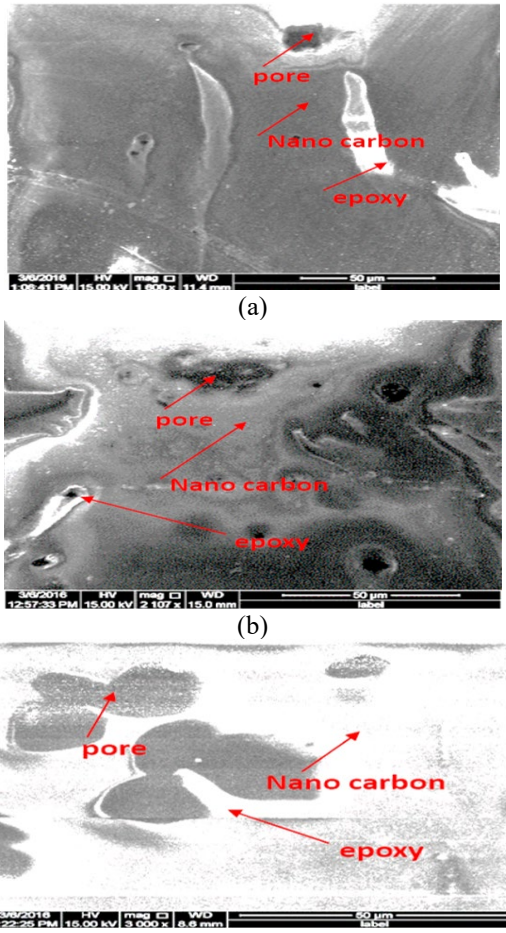

Fig. 2. SEM result for epoxy/MWCNTs nano-composite plate at various weight ratios of MWCNTs; (a) 0.1 wt.% MWCNTs, (b) 0.5 wt.% MWCNTs, and (c) 1 wt.% MWCNTs

2.3 Tensile Tests

The samples of tensile tests were prepared utilizing a CNC machine. And, four series of standard samples were arranged: Pure epoxy, nano composite plate with 0.1, 0.5 and 1 wt.% of MWCNT, respectively according to the standard ASTM D638. Tensile tests were carried out using a servo-hydraulic Tinius Olsen H50KT at the room temperature as well as 5.0 mm/min cross-head speed.

3. THEORITICAL CONSIDRATIONS

3.1 Higher-Order Shear Deformation Plate Theory

The first three natural frequencies can be estimated by using HSPT. This theory can be developed from the assumption of classical laminate plate theory that the straight line, which is perpendicular to the midille surface before the deformation, becomes a curved line after the deformation, as shown in Fig. 3 (Jones, 1975; Voyiadjis and Kattan, 2005).

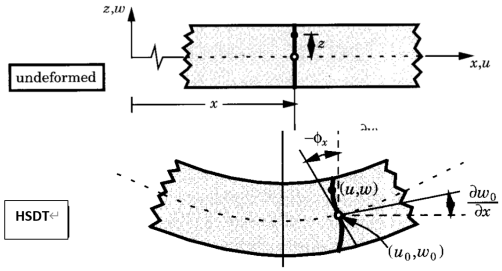

Fig. 3. The principle of HSPT (Reddy, 2004)

The displacement field is (Reddy, 2004):

$$u(x,y,z,t)=u_o(x,y,t)+z\ \emptyset_x(x,y,t) - \frac{4}{3h^2}\ z^3\left(\ \emptyset_x+\ \frac{\partial w_0}{\partial x}\ \right) \quad (1)$$

$$v(x,y,z,t)=v_o(x,y,t)+z\ \emptyset_y(x,y,t) - \frac{4}{3h^2}\ z^3\left(\ \emptyset_y+\ \frac{\partial w_0}{\partial y}\ \right) \quad (2)$$

$$w(x,y,z,t)=w_o(x,y,t) \quad (3)$$

The motion equation being derived based on the variation principle of Hamilton, and the equation of motion for free vibation are listed below (Reddy,2004)

$$\delta u_0 : \frac{\partial N_{xx}}{\partial x}+\frac{\partial N_{xy}}{\partial y} = I_0\ddot{u_0}+J_0\ddot{\emptyset}_x - c_1 I_3\frac{\partial \ddot{w}_0}{\partial x} \quad (4)$$

$$\delta v_0 : \frac{\partial N_{xy}}{\partial x}+\frac{\partial N_{yy}}{\partial y} = I_0\ddot{v_0}+J_0\ddot{\emptyset}_y - c_1 I_3\frac{\partial \ddot{w}_0}{\partial y} \quad (5)$$

$$\delta w_0 : \frac{\partial Q_x}{\partial x} - c_2\frac{\partial R_x}{\partial x} + \frac{\partial Q_y}{\partial y} - c_2\frac{\partial R_y}{\partial y} + c_1\left(\frac{\partial^2 P_{xx}}{\partial x^2} + 2\frac{\partial^2 P_{xy}}{\partial x\,\partial y} + \frac{\partial^2 P_{yy}}{\partial y^2} + N_{xx}\frac{\partial^2 w}{\partial x^2} + N_{yy}\frac{\partial^2 w}{\partial y^2} + 2N_{xy}\frac{\partial^2 w}{\partial x \partial y}\right) = I_0\ddot{w}_0 - c_1^2 I_6\left(\frac{\partial^2 \ddot{w}_0}{\partial x^2}+\frac{\partial^2 \ddot{w}_0}{\partial y^2}\right) + c_1\left[I_3\left(\frac{\partial \ddot{u}_0}{\partial x}+\frac{\partial \ddot{v}_0}{\partial y}\right) + J_4\left(\frac{\partial \ddot{\emptyset}_x}{\partial x}+\frac{\partial \ddot{\emptyset}_y}{\partial y}\right)\right] \quad (6)$$

$$\delta\emptyset_x : \frac{\partial M_{xx}}{\partial x} - c_1\frac{\partial P_{xx}}{\partial x} + \frac{\partial M_{xy}}{\partial y} - c_1\frac{\partial P_{xy}}{\partial y} - Q_x + c_2 R_x = J_1\ddot{u_0} + K_2\ddot{\emptyset}_x - c_1 J_4\frac{\partial \ddot{w}_0}{\partial y} \quad (7)$$

$$\delta\emptyset_y : \frac{\partial M_{xy}}{\partial x} - c_1\frac{\partial P_{xy}}{\partial x} + \frac{\partial M_{yy}}{\partial y} - c_1\frac{\partial P_{yy}}{\partial y} - Q_y + c_2 R_y = J_1\ddot{v_0} + K_2\ddot{\emptyset}_y - c_1 J_4\frac{\partial \ddot{w}_0}{\partial y} \quad (8)$$

Where, the variables in these equations can be described

for single layer isotropic plates:

($B_{ij} = E_{ij} = 0$) and eliminated from the below equations give,

$$\begin{Bmatrix} N_{xx} \\ N_{yy} \\ N_{xy} \end{Bmatrix} = \begin{bmatrix} A_{11} & A_{12} & 0 \\ A_{12} & A_{22} & 0 \\ 0 & 0 & A_{66} \end{bmatrix} \begin{Bmatrix} \varepsilon^0_{xy} \\ \varepsilon^0_{xy} \\ \gamma^0_{xy} \end{Bmatrix} \quad (9)$$

$$\begin{Bmatrix} M_{xx} \\ M_{yy} \\ M_{xy} \end{Bmatrix} = \begin{bmatrix} D_{11} & D_{12} & 0 \\ D_{12} & D_{22} & 0 \\ 0 & 0 & D_{66} \end{bmatrix} \begin{Bmatrix} \varepsilon^1_{xx} \\ \varepsilon^1_{yy} \\ \gamma^1_{xy} \end{Bmatrix} - c_1 \begin{bmatrix} F_{11} & F_{12} & 0 \\ F_{12} & F_{22} & 0 \\ 0 & 0 & F_{66} \end{bmatrix} \begin{Bmatrix} \varepsilon^{(3)}_{xx} \\ \varepsilon^{(3)}_{yy} \\ \gamma^{(3)}_{xy} \end{Bmatrix} \quad (10)$$

$$\begin{Bmatrix} P_{xx} \\ P_{yy} \\ P_{xy} \end{Bmatrix} = + \begin{bmatrix} F_{11} & F_{12} & 0 \\ F_{12} & F_{22} & 0 \\ 0 & 0 & F_{66} \end{bmatrix} \begin{Bmatrix} \varepsilon^1_{xx} \\ \varepsilon^1_{yy} \\ \gamma^1_{xy} \end{Bmatrix} - c_1 \begin{bmatrix} H_{11} & H_{12} & 0 \\ H_{12} & H_{22} & 0 \\ 0 & 0 & H_{66} \end{bmatrix} \begin{Bmatrix} \varepsilon^{(3)}_{xx} \\ \varepsilon^{(3)}_{yy} \\ \gamma^{(3)}_{xy} \end{Bmatrix} \quad (11)$$

$$\begin{Bmatrix} Q_{yz} \\ Q_{xz} \end{Bmatrix} = \begin{bmatrix} A_{44} & 0 \\ 0 & A_{55} \end{bmatrix} \begin{Bmatrix} \gamma^{(0)}_{yz} \\ \gamma^{(0)}_{xz} \end{Bmatrix} - c_2 \begin{bmatrix} D_{44} & 0 \\ 0 & D_{55} \end{bmatrix} \begin{Bmatrix} \gamma^{(2)}_{yz} \\ \gamma^{(2)}_{xz} \end{Bmatrix} \quad (12)$$

$$\begin{Bmatrix} R_{yz} \\ R_{xz} \end{Bmatrix} = \begin{bmatrix} D_{44} & 0 \\ 0 & D_{55} \end{bmatrix} \begin{Bmatrix} \gamma^{(0)}_{yz} \\ \gamma^{(0)}_{xz} \end{Bmatrix} - c_2 \begin{bmatrix} F_{44} & 0 \\ 0 & F_{55} \end{bmatrix} \begin{Bmatrix} \gamma^{(2)}_{yz} \\ \gamma^{(2)}_{xz} \end{Bmatrix} \quad (13)$$

Where:

$$A_{ij},\ B_{ij},\ D_{ij},\ E_{ij},\ F_{ij},\ H_{ij} = \int_{-h/2}^{h/2} Q_{ij}\ (1,\ z,\ z^2,\ z^3,\ z^4,\ z^6)\ dz \quad (14)$$

$$Q_{ij} = \begin{bmatrix} \frac{E}{1-v^2} & \frac{vE}{1-v^2} & 0 \\ \frac{vE}{1-v^2} & \frac{E}{1-v^2} & 0 \\ 0 & 0 & \frac{E}{2(1+v)} \end{bmatrix} \quad (15)$$

$$(I_0, I_1. I_2, I_3, I_4. I_5, I_6) = \int_{-h/2}^{h/2} \rho(1, z, z^2, z^3, z^4, z^5, z^6) dz \quad (16)$$

$$c_2 = 3c_1;\ c_1 = 4/3h^2 \quad (17)$$

$$J_i = I_i - c_1 I_{i+2}\ ,\ K_2 = I_2 - 2c_1 I_4 + c_1^2 I_6 \quad (18)$$

For rectangular nano-composite plate with edges y = (0, b), x = (0, a) simply supported, Navier solution is used. By assuming the subsequent displacement representation (Reddy, 2004):

$$u_0(x,y,t) = \sum_{n=1}^{\infty} \sum_{m=1}^{\infty} U_{mn}\, e^{-i\omega t} cos\frac{m\pi}{a}x\ sin\frac{n\pi}{b}y \quad (19\text{-a})$$

$$v_0(x,y,t) = \sum_{n=1}^{\infty} \sum_{m=1}^{\infty} V_{mn}\, e^{-i\omega t} sin\frac{m\pi}{a}x\ cos\frac{n\pi}{b}y \quad (19\text{-b})$$

$$w_0(x,y,t) = \sum_{n=1}^{\infty} \sum_{m=1}^{\infty} W_{mn}\, e^{-i\omega t} sin\frac{m\pi}{a}x\ sin\frac{n\pi}{b}y \quad (19\text{-c})$$

$$\emptyset_x(x,y,t) = \sum_{n=1}^{\infty} \sum_{m=1}^{\infty} X_{mn}\, e^{-i\omega t} cos\frac{m\pi}{a}x\ sin\frac{n\pi}{b}y \quad (19\text{-d})$$

$$\emptyset_y(x,y,t) = \sum_{n=1}^{\infty} \sum_{m=1}^{\infty} Y_{mn}\, e^{-i\omega t} sin\frac{m\pi}{a}x\ cos\frac{n\pi}{b}y \quad (19\text{-e})$$

Where, m is the no. of half wavelengths in the x-direction (m = 1, 2 and 3), and n is the no. of half wavelengths in the y-direction (n = 1, 2 and 3). U_{mn}, V_{mn}, W_{mn}, X_{mn}, Y_{mn} are arbitrary constants to be determined; to solve the above nonlinear equations; the stress function ψ(x,y.t) is introduced as (Pham et al., 2016):

$$N_{xx} = \frac{\partial^2 \psi}{\partial y^2}\ N_{yy} = \frac{\partial^2 \psi}{\partial x^2}\ N_{xy} = -\frac{\partial^2 \psi}{\partial x\, \partial y} \quad (20)$$

Then, substituting Equation 19 into the Equations 4 and 5 yields:

$$\ddot{u}_0 = \frac{c_1 I_3}{I_0}\frac{\partial \ddot{w}}{\partial x} - \frac{J_1}{I_0}\ddot{\emptyset}_x \quad (21)$$

$$\ddot{v}_0 = \frac{c_1 I_3}{I_0}\frac{\partial \ddot{w}}{\partial y} - \frac{J_1}{I_0}\ddot{\emptyset}_y \quad (22)$$

Then, substituting Equations 20, 21 and 22 into Equations 6, 7 and 8 to obtain:

$$\delta w_0 : \frac{\partial Q_x}{\partial x} - c_2\frac{\partial R_x}{\partial x} + \frac{\partial Q_y}{\partial y} - c_2\frac{\partial R_y}{\partial y} + c_1\left(\frac{\partial^2 P_{xx}}{\partial x^2} + 2\frac{\partial^2 P_{xy}}{\partial x\, \partial y} + \frac{\partial^2 P_{yy}}{\partial y^2} + \frac{\partial^2 \psi}{\partial y^2}\frac{\partial^2 w}{\partial x^2} + \frac{\partial^2 \psi}{\partial x^2}\frac{\partial^2 w}{\partial y^2} - 2\frac{\partial^2 \psi}{\partial x\, \partial y}\frac{\partial^2 w}{\partial x \partial y}\right) = I_0\ddot{w}_0 - c_1^2 I_6\left(\frac{\partial^2 \ddot{w}_0}{\partial x^2} + \frac{\partial^2 \ddot{w}_0}{\partial y^2}\right) + c_1\left[I_3\left(\frac{\partial}{\partial x}\left(\frac{c_1 I_3}{I_0}\frac{\partial \ddot{w}}{\partial x} - \frac{J_1}{I_0}\ddot{\emptyset}_x\right) + \frac{\partial}{\partial y}\left(\frac{c_1 I_3}{I_0}\frac{\partial \ddot{w}}{\partial y} - \frac{J_1}{I_0}\ddot{\emptyset}_y\right)\right) + J_4\left(\frac{\partial \ddot{\emptyset}_x}{\partial x} + \frac{\partial \ddot{\emptyset}_y}{\partial y}\right)\right] \quad (23)$$

$$\delta\emptyset_x : \frac{\partial M_{xx}}{\partial x} - c_1\frac{\partial P_{xx}}{\partial x} + \frac{\partial M_{xy}}{\partial y} - c_1\frac{\partial P_{xy}}{\partial y} - Q_x + c_2 R_x = J_1\frac{c_1 I_3}{I_0}\frac{\partial \ddot{w}}{\partial x} - \frac{J_1 J_1}{I_0}\ddot{\emptyset}_x + K_2\ddot{\emptyset}_x - c_1 J_4\frac{\partial \ddot{w}_0}{\partial y} \quad (24)$$

$$\delta\emptyset_y : \frac{\partial M_{xy}}{\partial x} - c_1\frac{\partial P_{xy}}{\partial x} + \frac{\partial M_{yy}}{\partial y} - c_1\frac{\partial P_{yy}}{\partial y} - Q_y + c_2 R_y = J_1\frac{c_1 I_3}{I_0}\frac{\partial \ddot{w}}{\partial y} - \frac{J_1 J_1}{I_0}\ddot{\emptyset}_y + K_2\ddot{\emptyset}_y - c_1 J_4\frac{\partial \ddot{w}_0}{\partial y} \quad (25)$$

Let ψ(x,y.t) as

$$\psi(x, y. t) = A_1 cos2\alpha x + A_2 cos2\beta y + A_3 sin\alpha x\ sin\beta y + \frac{1}{2}N_{xo}y^2 + \frac{1}{2}N_{yo}x^2 \quad (26)$$

Where, $N_{xo} and\ N_{yo}$ are buckling load and here is set to zero. A_1, A_2, A_3 are arbitrary constants and are found by substituting Equation 26 into the compatibility equation of one layer isotropic as (Pham et al., 2016):

$$\frac{1}{A_{11}(1-v^2)}\left(\frac{\partial^4 \psi}{\partial x^4} + 2\frac{\partial^4 \psi}{\partial x^2 \partial y^2} + \frac{\partial^4 \psi}{\partial y^4}\right) = \left(\frac{\partial^2 w}{\partial x \partial y}\right)^2 - \frac{\partial^2 w}{\partial x^2}\frac{\partial^2 w}{\partial y^2} \quad (27)$$

The yield constants are:

$$A_1 = \frac{\beta^2 A_{11}(1-\nu^2)}{4(16\alpha^2+16)} W_{mn} \quad (28)$$

$$A_2 = \frac{\alpha^2 A_{11}(1-\nu^2)}{4(-16\beta^2-4)} W_{mn} \quad (29)$$

$$A_3 = -\frac{\alpha^2\beta^2 A_{11}(1-\nu^2)}{\alpha^4+\alpha^2\beta^2-\beta^4} W_{mn} \quad (30)$$

Solving for linear equation, the natural frequency can be found from:

$$[k] + [m]w^2 = 0 \quad (31)$$

$$|k + mw^2| = D \rightarrow |D| = 0 \quad (32)$$

All factors in determents are derived using Navier solution with stress function and coded in MATLAB software.

3.2 Numerical Analysis

3.2.1 Element Selection and Modeling

The technique of finite element was used for analyzing free vibration of nano composite plate. And, a model was built in ANSYS 15.0 utilizing the element named (shell 281), as displayed in Fig. 4. For every node, there are six degrees of freedom (D.O.F.): Three translations in the global coordinates (X, Y, Z) and three rotational DOF about the x, y and z axes. It may be utilized to model the layered uses, and it comprises the transverse shear deformation effect. And, the accurateness of this element is equal to the FSDT. There were three steps for modeling in ANSYS 15.0:

1. Constructing the model: It comprises defining the type of element, properties of material (Young's modulus as well as Poison's ratio) and creating the models.
2. Modal analysis solution: It includes the boundary conditions and the solving analysis.
3. Postprocessor: It comprises listing the natural frequency results and showing the mode shape.

3.2.2 Mesh Convergence

The study of convergence was achieved for finding the suitable mesh to be employed in the free vibration analysis of nano-composite plate. The meshes were performed by raising the elements no. in the x and y directions, and the natural frequencies for each of such cases are evinced in Fig. 5. When the D.O.F. is increased from 576 to 2046, and the discrepancy in natural frequency is only about 0.24%. The too small discrepancy noted between the D.O.F. 2046 and the D.O.F. 4416 is 0.00346%. And, no discrepancy was observed between the D.O.F. 4416 and the D.O.F. 7686. Also, the natural frequency for each of such models is elucidated in Table 1. And, this denotes that the D.O.F. 4416 is able to perform the analysis within a practical accuracy degree.

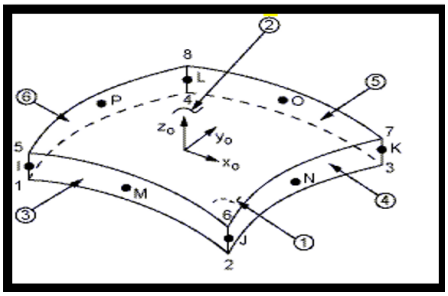

Fig. 4. Shell 281 geometry (ANSYS 15)

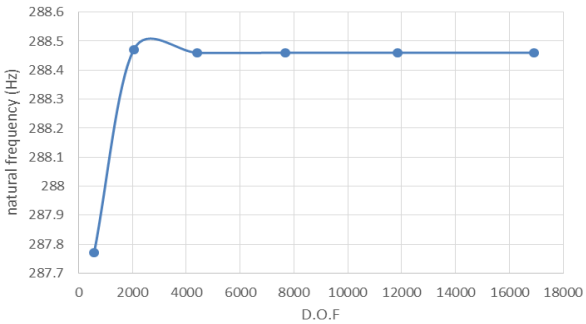

Fig. 5. The convergence study of natural frequency vs. D.O.F. for the S-S-S-S plate (pure epoxy)

Table 1. The convergence study of natural frequency for the S-S-S-S plate (pure epoxy) with a = b, h = 2 mm

No. of element	No. of node	D.O.F	Natural frequency (Hz)
25	96	576	287.77
100	341	2046	288.47
225	736	4416	288.46
400	1281	7686	288.46
625	1976	11856	288.46
900	2821	16926	288.46

4. RESULT AND DISCUSSION

4.1 Tensile Test Results

It can be shown from the experimental results of stress strain curves in Fig. 6, the nano-composite with 0.1% weight ratio has the maximum enhancement in the stress strain curves. The details of the mechanical properties can be shown in Table 2 such as the Young's modulus is somewhat increased via 7% as the supplement of filler is increased; the ultimate raising in Young's modulus is 26% if the weight percentage of nano carbon is 1% compared with the pure epoxy sample; this increasing is depended upon the nano carbon's clusters dimension as well as their spreading into the matrix of epoxy matrix. And, the maximum tensile strength has an ultimate value of 30.448 MPa at the weight ratio 0.1 wt.%, and it can be seen for 0.1% weight ratio that there is less voids have been noted

from the images of SEM Fig. 2 achieved in the current investigation. Also, the ultimate elongations were reduced as the weight ratio of MWCNT values were augmented due to that the creation of attractive polar forces and Van der Waals bonding the nanotubes with epoxy led to decrease the epoxy chains length and the free volume space, as well as achieved the reduction of maximum strength and ultimate elongation.

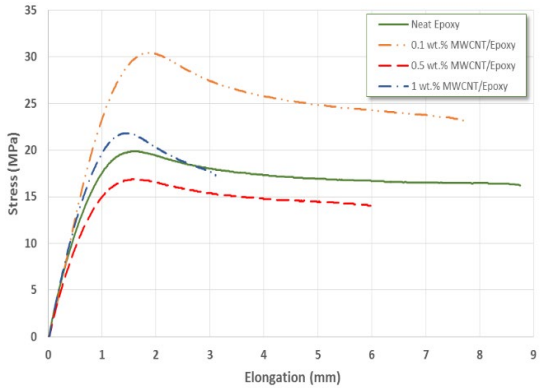

Fig. 6. Stress-Strain behaviors of the MWCNT/Epoxy nano-composites with various weight ratios

Table 2. The mechanical properties of nano-composites plate

	Young's modulus (GPa)	Ultimate strength (MPa)	Maximum elongation (%)
Epoxy	6.9	19.9	3.51
Epoxy + 0.1 wt% MWCNT	7.3	31	3.13
Epoxy + 0.5 wt% MWCNT	8.3	17	2.45
Epoxy + 1.0 wt% MWCNT	8.6	21	1.25

4.2 Vibration Results

4.2.1 Verification of Case Studies

In the current research, a series of preselected cases was modeled for verifying the accurateness of the technique of analysis. And, the outcomes of Shooshtari and Rafiee (2011) were compared to analytical solution and numerical solution (ANSYS), as depicted in Table 3. From the outcomes listed in this table, it's clear that the solution approaches give better outcomes for analytical solution than numerical one for maximum error 3.9% for analytical solution.

4.2.2 Natural Frequency (for Different Loading Ratios)

The first three natural frequencies for simply supports composite plate with thickness h = 1 mm and equal length (a) and width (b) are listed in Table 4 (analytically and numerically). From this table, the results manifest that the plate without any filler (pure epoxy) has the minimum frequencies compared with the composite plate consisting of nano carbon with epoxy resin, because the mechanical property (Young's modulus) increased higher than the increasing in density when adding the CNT to the epoxy resin. When the loading ratio became 0.1%, the fundamental natural frequency rose by 2.6%. If the loading ratio is increased from 0.1% to 0.5%, the frequency augmented by 5.9%. And, increasing the load ratio from 0.5% to 1% led to raise the frequency with 1.9%. The above increasing in frequency is due to the rise in the mechanical properties that led to an increase in the stiffness matrix. The maximum discrepancy between numerical and analytical results is 2% at a load ratio of 1%, and it can be seen that the frequency obtained from HSPT has lower value than ANSYS software because of the considered shear effect. The three mode shapes are revealed in Fig. 7. Also, the three mode shapes for the four types of nano-composite plate in ANSYS are depicted in Fig. 8.

Table 3. Three fundamental frequencies of simply supported nano composite plate with different loading ratios of CNTs, $\bar{\Omega} = \Omega \frac{a^2}{h}\sqrt{\frac{\rho_0}{E_0}}$ compared with ref (Shooshtari and Rafiee, 2011)

Loading ratio	w_1 ref	w_1 (HSPT) (Error%)	w_1 (ANSYS) (Error%)	w_2 ref	w_2 (HSPT) (Error%)	w_2 (ANSYS) (Error%)	w_3 ref	w_3 (HSPT) (Error%)	w_3 (ANSYS) (Error%)
0.12	15.69	16.2 (3%)	17 (8%)	20.09	20.9 (4%)	21.4 (6%)	31.29	32.5 (3.9%)	27.4 (12%)
0.17	19.2	19.5 (1.6%)	20.8 (8%)	25.17	25.5 (1.3%)	24.4 (3%)	39.9	41 (2.8%)	35 (12%)
0.28	22.94	23.3 (1.56%)	24.2 (5%)	28.47	29 (1.9%)	25.96 (9.8%)	43.1	44 (2%)	39 (9.5%)

Table 4. Three Natural frequencies (Hz) for S-S-S-S plate with a = b, h = 1 mm and different loading ratios of CNTs

Loading ratio	w_1 ANSYS	w_1 HSPT	w_2 ANSYS	w_2 HSPT	w_3 ANSYS	w_3 HSPT
Pure epoxy	245.224	240	613.7	600	613.7	602
0.1%	251.7	246.7	630.99	625	630.99	628
0.5%	266.599	262	667.235	659.8	667.235	664
1%	271.537	266	679.595	671	679.595	675

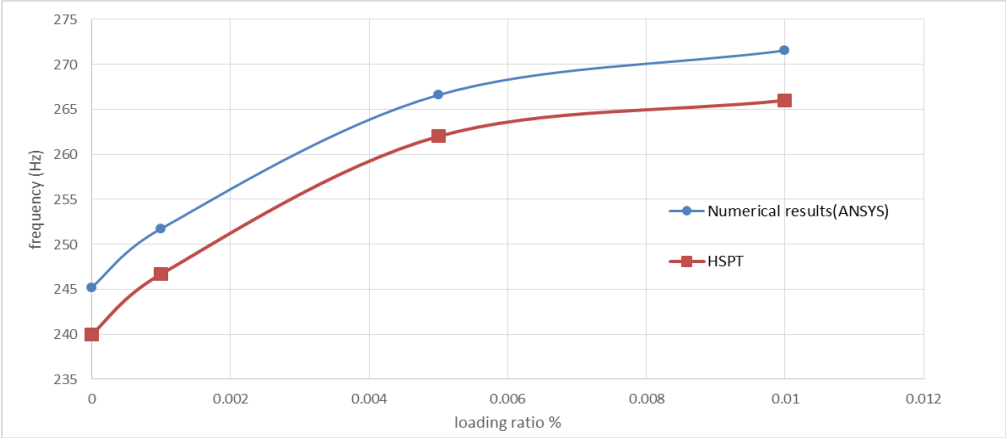

Fig. 7. Loading ratio effect on the natural frequency of S-S-S-S plate

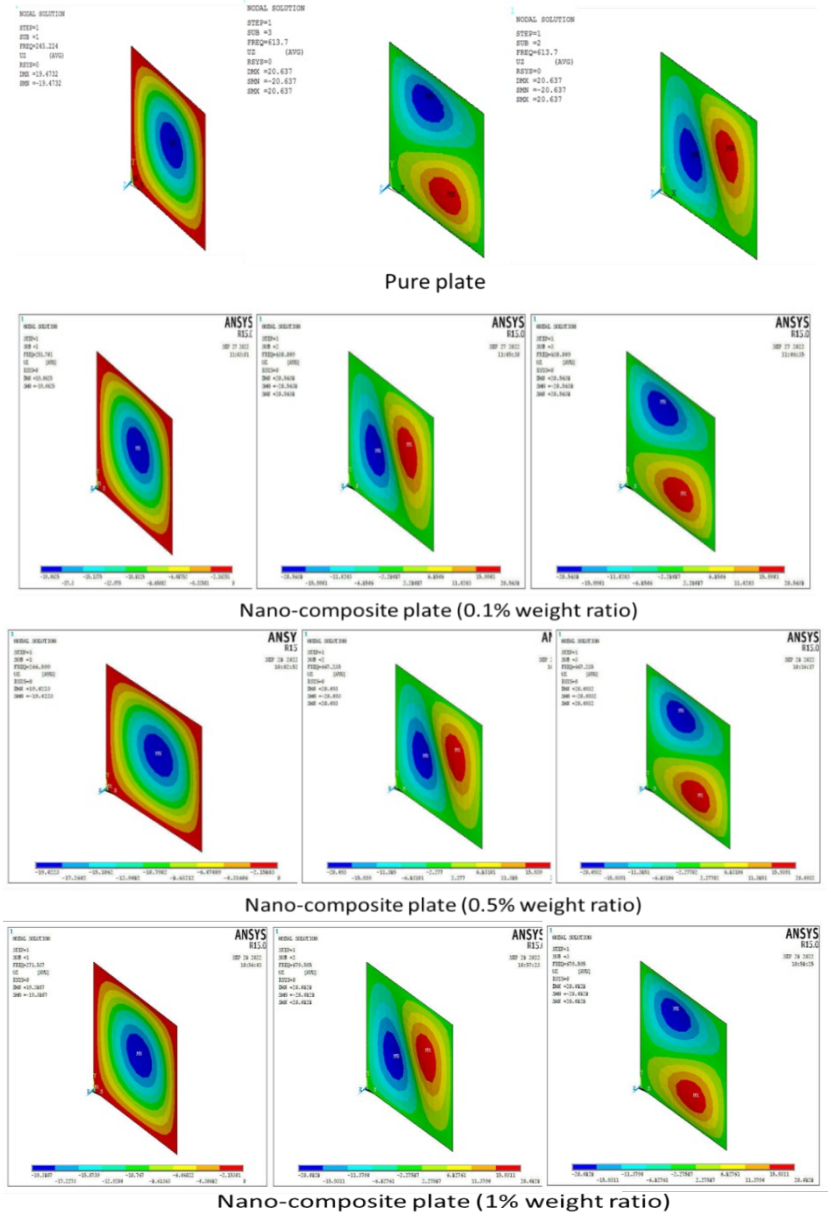

Fig. 8. Three mode shapes for the four types of nano-composite in ANSYS

4.2.3 Aspect Ratio

Figs. 9 and 10 for S-S-S-S nano composite plates with thickness 1 mm and for different lading ratios elucidate that the natural frequency reduces when a/b increases with a high percentage that reaches to 59.9% if the aspect ratio raises from 0.5 to 1 in 0.5% weight ratio. From the other side, when a/b changes from 0.5 to 1, in the composite plate with loading ratio 1 wt.%, the decreasing in natural frequency is 28%. When the aspect ratio rises from 1 to 1.5, the decreasing ratio is 27%, and the deceasing is 13% for the increase of aspect ratio from 1.5 to 2. This decrease is according to the raising in mass matrix that led to a decrease in the natural frequency. The maximum discrepancy can be occurred at 1.5 aspect ratio of pure plate with 10.4%.

4.2.4 Thickness Ratio

It can be observed from Figs. 11 and 12 that the natural frequency for S-S-S-S nano-composite plate decreases when the thickness ratio increases with percentage 47.7% for all cases and when the thickness ratio rises from 10 to 20. If the thickness ratio increases from 20 to 30, the natural frequency decreases by 33%. And, the decreasing ration is 24% for increasing the thickness ratio from 30 to 40. The maximum discrepancy is 10% at thickness ratio 20 for pure plate.

The main contribution of this work is compared four different percentages of nano carbon tube (0, 0.1%, 0.5%, 1%) based on natural frequency and mechanical properties. The best mechanical properties are found experiment from 0.1% weight ratio. The vibration analysis is studied theoretically by utilizing HSPT and numerically by ANSYS software. The stress function ψ(x,y.t) is introduced to solve the nonlinearity of HSPT. The maximum increasing in natural frequency due to increasing in loading ratio from 0.1 wt.% to 0.5 wt.% is 5.9%.

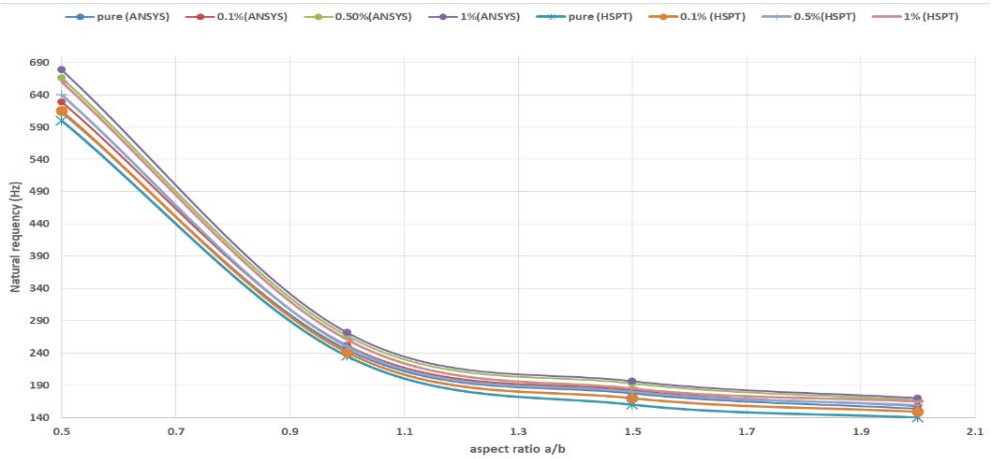

Fig. 9. Effect of aspect ratio on the natural frequency for S-S-S-S nano-composite plate

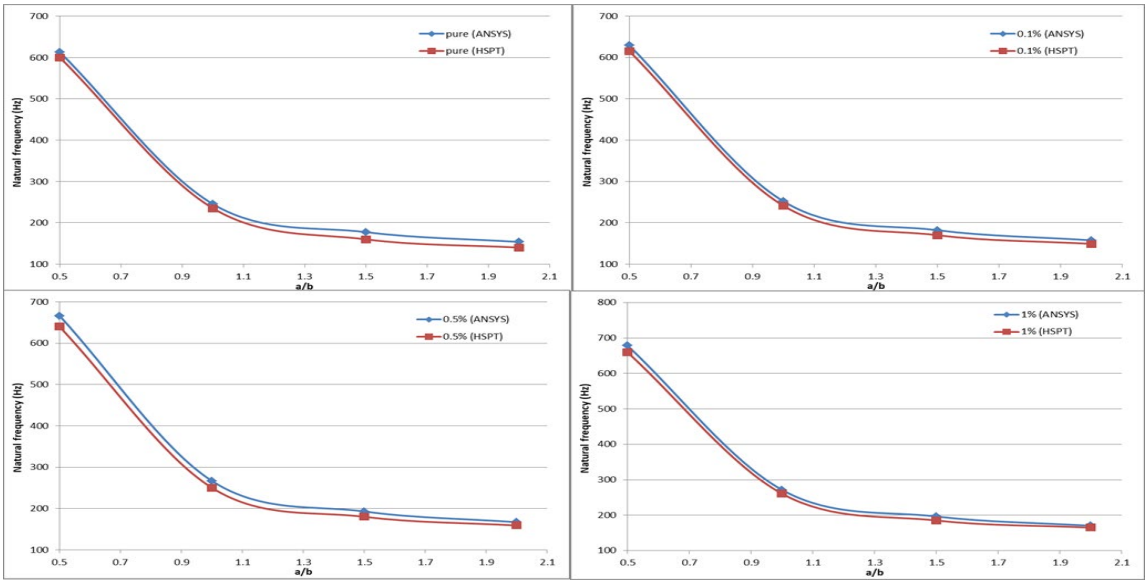

Fig. 10. Detailed curves for the relation between aspect ratio and natural frequency

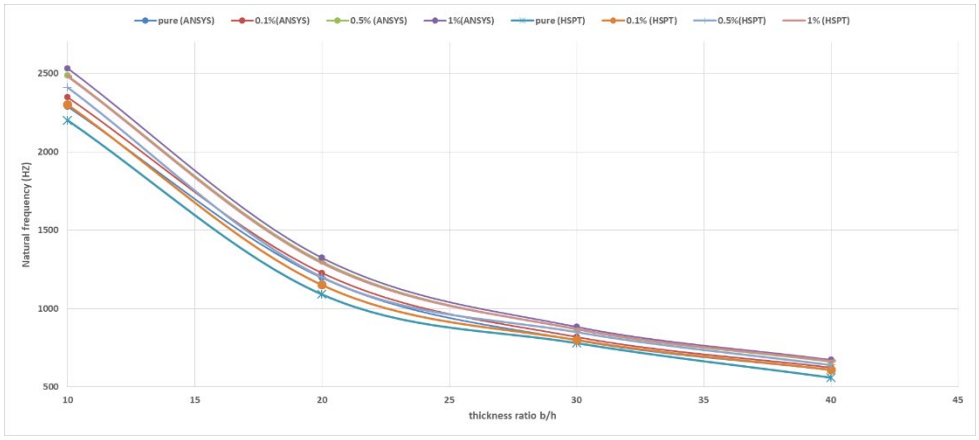

Fig. 11. Effect of thickness ratio on the natural frequency for S-S-S-S nano-composite plate

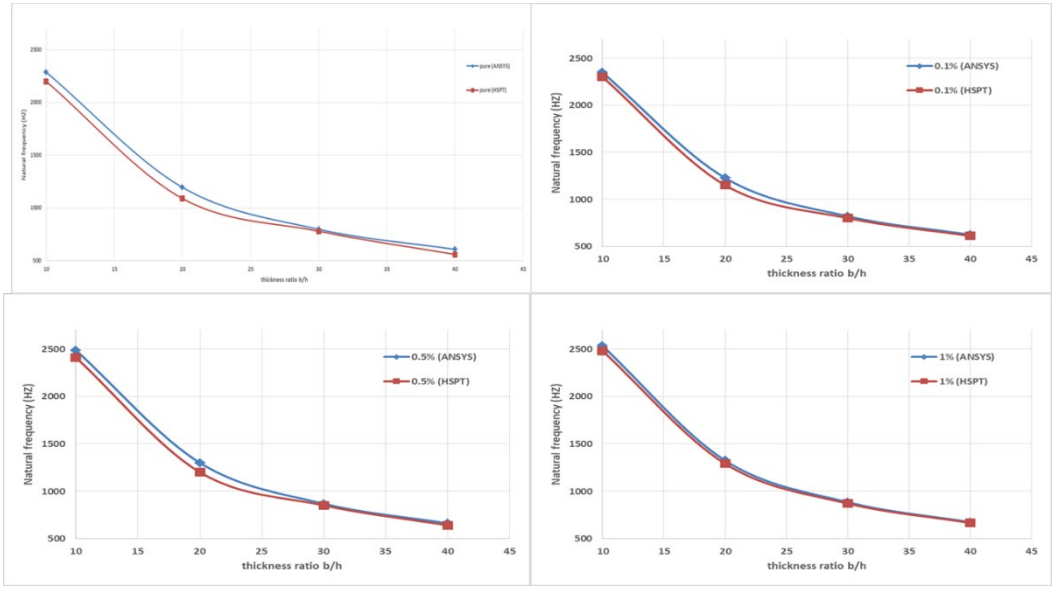

Fig. 12. Detailed curves for the relation between thickness ratio and natural frequency

5. CONCLUSION

In the present research, the mechanical properties of MWCNT/Epoxy nano-composites at various load ratios (0.1, 0.5 and 1 wt.%) were experimentally considered. MWCNTs were added to epoxy by a magnetic stirrer to form the nano-composite plate. Dispersion of the MWCNTs into the epoxy resin had highly affected on the mechanical tests' outcomes, and it was manifested by SEM. The low weight fractions of MWCNT (at 0.1 and 0.5 wt.%, respectively) can improve the tensile properties of the nano-composites. The effect of adding nano carbon tube to epoxy resin was studied theoretically by utilizing HSPT and numerically by ANSYS software. The equation of motion was first derived analytically, then the stress function was applied to deal with the non-linearity of equations, and finally the Navier solution was implemented to find the natural frequency; the maximum discrepancy can be occurred at 1.5 aspect ratio of pure plate with 10.4%. The maximum increasing in natural frequency due to increasing in loading ratio from 0.1% to 0.5% is 5.9%. The increasing of thickness ratio and aspect ratio may decrease the fundamental natural frequency by 47% and 59.9%, respectively. Above the aspect ratio 1.5, the natural frequency becomes stable and has a small change with increasing natural frequency.

REFERENCES

Ahmadi, M., Ansari, R., Rouhi, H. 2019. Free and forced vibration analysis of rectangular/circular/annular plates made of carbon fiber-carbon nanotube-polymer hybrid composites. Science and Engineering of Composite Materials, 26, 70–76.

Bastami, M., Behjat, B. 2017. Ritz solution of buckling and vibration problem of nanoplates embedded in an elastic medium. Sigma Journal of Engineering and Natural Sciences, 35, 285–302.

Bouazza, M., Zenkour, A.M. 2020. Vibration of carbon nanotube-reinforced plates via refined n th-higher-order theory. Archive of Applied Mechanics, 90, 1755–1769.

Chakravety, S. 2008.Vibration of plates. CRC Press.

Civalek, Ö., Akbaş, Ş.D., Akgöz, B., Dastjerdi, S. 2021. Forced vibration analysis of composite beams reinforced by carbon nanotubes. Nanomaterials, 11, 571.

Cong, P.H., Anh, V.M., Duc, N.D. 2017. Nonlinear dynamic response of eccentrically stiffened FGM plate using Reddy's TSDT in thermal environment. Journal of Thermal Stresses, 40, 704–732.

Ebrahimi, F. (Ed.). 2012. Nanocomposites: New trends and developments. BoD–Books on Demand.

Ebrahimi, F., Dabbagh, A. 2019. Vibration analysis of multi-scale hybrid nanocomposite plates based on a Halpin-Tsai homogenization model. Composites Part B: Engineering, 173, 106955.

Hocaoğlu, M., Karagülle, H. 2020. Effect of carbon nanotube reinforcement on the natural frequencies and damping ratios of nanocomposite beams. Materials Research Express, 7, 025021.

Jones, R.M. 1975. Mechanics of Composite Materials, McGraw-Hill, New York.

Maji, P., Rout, M., Karmakar, A. 2022. The free vibration response of temperature-dependent carbon nanotube-reinforced composite stiffened plate. Mechanics of Advanced Materials and Structures, 29, 2555–2569.

Melaibari, A., Daikh, A.A., Basha, M., Abdalla, A.W., Othman, R., Almitani, K.H., Hamed, M.A., Abdelrahman, A., Eltaher, M.A. 2022. Free vibration of FG-CNTRCs nano-plates/shells with temperature-dependent properties. Mathematics, 10, 583.

Mohammadimehr, M., Rostami, R. 2017. Bending, buckling, and forced vibration analyses of nonlocal nanocomposite microplate using TSDT considering MEE properties dependent to various volume fractions of $CoFe_2O_4$-$BaTiO_3$. Journal of Theoretical and Applied Mechanics, 55.

Pan, S., Feng, J., Safaei, B., Qin, Z., Chu, F., Hui, D. 2022. A comparative experimental study on damping properties of epoxy nanocomposite beams reinforced with carbon nanotubes and graphene nanoplatelets. Nanotechnology Reviews, 11, 1658–1669.

Parameswaranpillai, J., Hameed, N., Kurian, T., Yu, Y. 2016. Nanocomposite materials: Synthesis, properties and applications. CRC Press.

Reddy, B.S., Kumar, J.S., Reddy, C.E., Reddy, K.V.K. 2015. Buckling analysis of functionally graded plates using higher order shear deformation theory with thickness stretching effect. International Journal of Applied Science and Engineering, 13, 19–35.

Reddy, J.N. 2003. Mechanics of laminated composite plates and shells: theory and analysis. CRC press.

Safaei, B., Ahmed, N.A., Fattahi, A.M. 2019. Free vibration analysis of polyethylene/CNT plates. The European Physical Journal Plus, 134, 271.

Shooshtari, A., Rafiee, M. 2011.Vibration characteristics of nanocomposite plates under thermal conditions including nonlinear effects. International Journal of Applied Research in Mechanical Engineering, 1, 60–68.

Theory, Analysis, and Element Manuals, ANSYS 15 software.

Voyiadjis, G.Z., Kattan, P.I. 2005. Mechanics of composite materials with MATLAB. Springer Science & Business Media.

Wu, H., Li, Y., Li, L., Kitipornchai, S., Wang, L., Yang, J. 2022. Free vibration analysis of functionally graded graphene nanocomposite beams partially in contact with fluid. Composite Structures, 291, 115609.

Xu, D., Ni, Z., Li, Y., Hu, Z., Tian, Y., Wang, B., Li, R. 2021. On the symplectic superposition method for free vibration of rectangular thin plates with mixed boundary constraints on an edge. Theoretical and Applied Mechanics Letters, 11, 100293.